Earthline Journal of Mathematical Sciences
E-ISSN: 2581-8147
Volume 14, Number 2, 2024, Pages 257-281
https://doi.org/10.34198/ejms.14224.257281

Magnetized Flow of Maxwell Fluid over a Slippery Stretching Reactive Surface with Thermophoretic Deposition

Peter Yakubu Pandam[1], Christian John Etwire[2], Golbert Aloliga[3,*] and Yakubu Ibrahim Seini[4]

[1] C. K. Tedam University of Technology and Applied Sciences, P. O. Box 24, Navrongo, Upper East Region, Ghana
e-mail: peterpandam@gmail.com

[2] C. K. Tedam University of Technology and Applied Sciences, P. O. Box 24, Navrongo, Upper East Region, Ghana
e-mail: jecpapa@yahoo.com

[3] C. K. Tedam University of Technology and Applied Sciences, P. O. Box 24, Navrongo, Upper East Region, Ghana
e-mail: aloligagolbert@gmail.com

[4] School of Engineering, University for Development Studies, Nyankpala Campus, Northern Region, Ghana
e-mail: yakubuseini@yahoo.com

Abstract

This manuscript investigated mathematically magnetized Maxwell fluid over slippery stretching reactive surface with thermophoretic deposition. Similarity transformation was used to recast partial differential equations modeling flow problem to nonlinear coupled ordinary differential equations which were solved using fourth order Range-Kutta method and Newton-Raphson shooting technique. Numerical results were compared with literature-based results and found to be in good accord. Skin friction coefficient, Nusselt number, Sherwood number, velocity profiles, temperature profiles and concentration profiles which are of importance to engineers, were found to be influenced by thermo-physical parameters governing the dynamics of flow. Their effects were illustrated in tabular form and graphically. The study found that increasing Thermophoretic deposition parameter, Momentum slip parameter and Biot number amplified rate of heat transfer but decreased rate of mass transfer and Skin friction coefficients. Thermal Grashof, Solutal

Received: September 14, 2023; Accepted: December 8, 2023; Published: January 10, 2024

2020 Mathematics Subject Classification: 76-10, 76A05, 76D05.

Keywords and phrases: magnetized flow, Maxwell fluid, slippery surface, thermophoretic deposition.

*Corresponding author

Grashof, and Damkohler numbers reduced skin friction coefficients but increased heat and mass transfer rates.

Nomenclature

(x, y)	Cartesian Coordinates	N_B	Buoyancy ratio parameter
(u, v)	velocity components	Br	Brinkman number
C_w	Concentration at wall	S_T	Thermal stratification parameter
C_∞	Free stream concentration	Do	Dufour number
C	chemical concentration species of fluid	Le	Lewis number
T	Temperature of fluid	β	Chemical reaction parameter
T_∞	Free stream temperature	S	Suction parameter
T_w	Wall Temperature	T	Thermophoresis
Gr	Grashof number	M	Magnetic field parameter
K	Permeability parameter		
Pr	Prandtl number		

Greek Letters		**Subscripts**	
μ	Coefficient of viscosity	∞	Condition at free stream
ρ	Fluid Density	W	Condition at wall
ϕ	Dimensionless concentration		
θ	Dimensionless temperature		
η	Dimensionless variable		
υ	Kinematic viscosity		
ψ	Stream function		

1. Introduction

Research in magnetized flow of Maxwell fluid over slippery stretching reactive surface with thermophoretic deposition continues to attract the researchers and scientists enthusiasm based on its engineering and industrial applications. Non-isothermal Maxwell fluid flow about fixed flat plate with a transverse magnetic field indicate that, fluid velocity decreased with respect to magnetic field parameter while increasing with a Deborah number, Heyhat *et al.* [1]. Unsteady Maxwell fluid flow on stretched surface with chemical reaction was revealed that the Maxwell parameter suppressed the velocity field while concentration increased with the Maxwell parameter, Mukhopadhyay *et al*. [2]. Stretching permeable plate with boundary slip and a non-uniform heat sink is a key

factor, Zheng *et al*. [3]. Investigation on boundary layer flow in a mixed convection system and transfer of heat across a vertical slender cylinder was noted that the series solutions were valid for all mixed convection parameter values, Ellahi *et al*. [4]. Studies on mixed convective viscoelastic fluid through stretching cylinder with heat transfer and thermal conductivity altered the temperature and velocity profiles, as well as their corresponding thickness of the boundary layer, Hayat *et al*. [5]. Mixed convection flow and transfer of heat on ferromagnetic fluid over a stretching sheet with partial slip effects showed that the temperature profile rose with a velocity slip parameter and ferromagnetic parameter, but decreased with buoyancy parameter and Prandtl number, Zeeshan *et al*. [6]. Keller Box technique on studies effects of non-uniform heat sink on stagnation point flow of MHD Casson nanofluid flow in exponentially stretching surface showed that thermal boundary thickness layer reduced with Prandtl number, Krishnaiah *et al*. [7]. Investigation of the heat transfer behaviour of momentum on Maxwell, Jeffery and Oldroyd-B nanofluids passing through a stretching surface with a non-uniform heat sink. The results showed that increasing the non-uniform heated source or sink parameter increased the thickness of the thermal boundary layer, Sandeep and Sulochana [8]. Effects of non-uniform heat source and thermal radiation on MHD stagnation point flow of Maxwell nanofluid on a linear stretching surface. It was discovered that thickness of velocity boundary layer increased with velocity ratio parameter but decreased with Maxwell and magnetic field parameters, Abdela and Shanker [9]. Effect of non-uniform heat sink on Magnetohydrodynamic Maxwell nanofluid flow over convectively heated stretched surface with chemical reaction and magnetic field parameters, the findings showed de-escalating velocity field, Sajiol [10]. MHD mixed convective flow in Maxwell nanofluid across porous vertically stretching sheet in presence of chemically reactive species indicated that Magnetic field parameter reduces velocity while increasing the temperature profiles, Dassie *et al*. [11]. Buoyancy-driven mixed convective flow of magnetized Maxwell fluid with homogeneous-heterogeneous reaction and convection boundary conditions changes heat transmission at bottom disk increased with stretching parameter and Prandtl number, but converse trend was observed at top disk, Hashmi *et al*. [12]. Radiative mixed convection flow of Maxwell nanofluid on a stretching cylinder with joule heating and heat sink influence indicates that increasing value of Maxwell parameter increased stress relaxation phenomena, which reduced flow properties of Nano fluid, Islam *et al*. [13]. In response to novel heat flux model, impact of slip on mixed convective heat transfer of magnetized UCM fluid through porous material was discovered that, rising thermal relaxation parameter resulted in increased heat transfer

rate, Shah *et al.* [14]. MHD flow on Maxwell fluid with thermophoresis deposition is of great importance when it comes to industrial production of goods such as roofing sheets, polymers, textiles just to mention few. Knowledge of thermophoresis deposition help industrial managers to decide what to produce and at what time will it be convenient for their equipment, Aliakbar *et al.* [15]. Numerical technique for Maxwell fluid MHD flow through a vertically stretched sheet with thermophoresis and chemical reaction, temperature was shown to raise with magnetic strength, porosity, Deborah value, thermal radiation, and Eckert number using spectral relaxation approach with Chebyshev pseudo-spectral collocation technique, Shateyi [16]. The presence of chemical reaction with Joule heating and mass transfer of thermophoretic MHD flow of Powell-Eyring fluid over vertically stretched sheet using Runge-Kutta method and analytical Homotopy Evaluation (HEM) showed that Buoyancy ratio, heat radiation, chemical reaction, and magnetic field factors were discovered to have a significant impact on the flow field, Khan *et al.* [17]. MHD flow of Maxwell fluid with nanomaterials base on exponential stretching surface using homotopy analysis method which revealed that temperature increased with Deborah number, Hartman number and Brownian motion whereas it decreased with the thermophoresis parameter and Prandtl number, Farooq *et al.* [18]. Features of thermophoretic molecules deposition in a thermally developed Maxwell fluid flow between two infinite stretched disks was found that increasing the parameter of thermophoresis velocity deposition reduces the concentration of nanoparticles, Yu-Minehu *et al.* [19]. A power-law fluctuation in the surface temperature or heat flux is investigated in relation to the problem of continuous, laminar, hydromagnetic heat transfer via mixed convection across a continuously stretched surface, Emad and Mohamed [20]. A discovery of mathematical analysis of the bi-phase hydrodynamics Taylor flow for a range of fluids through a conduit was investigated by Abiev [21]. The impacts of non-Newtonian fluid electro-viscous flow in a channel with slip condition at greater zeta potential were studied by Banerjee *et al.* [22]. A parametric analysis of the fluid flow of microorganisms between a rotational disk and a cone was made by Alrabaiah *et al.* [23]. The dynamics of swimming microorganisms and water-based nanofluid flow on a Riga plate with the influence of thermal source and sink were investigated by Madhukesh *et al.* [24]. They estimated that the increase in slip effects has decreased the profiles of fluid concentration, temperature, and velocity. The mathematical model of bioconvective time-based nanofluid flow on a surface with nonlinear radiations has been quantitatively shown by Azam [25], who also investigated how fluid motion has degraded due to an increase in the bioconvective Rayleigh number.

In order to study the effects of bio-convection and activation energy on chemically reactive nanofluid flow utilizing nonlinear radiative effects, a new mathematical model was developed by Azam *et al.* [26]. Dissipative and Joule heating effects to study bio-convective MHD stratified nanofluid flow supported by gyrating and elongating sheet was investigated by Waqas *et al.* [27]. Another investigation of the stratified flow of a non-Newtonian Casson fluid including microorganisms on a stretching sheet with activation energy was carried out by Showkat *et al.* [28]. The distribution of the Casson fluid flows velocity decreases as the Casson and magnetic factors rise.

In the light of literature reviewed, the study on magnetized flow of Maxwell fluid on slippery stretching reactive surface with thermophoretic deposition is limited. Hence, the need of this study.

2. Formulation of Mathematical Model

Consider steady laminar incompressible two-dimensional flow of electrical conducting and chemically reacting Maxwell fluid over slippery reactive stretching permeable plate with thermophoretic deposition. The flow is subject to external magnetic field of strength B_0. Induced magnetic field influence is ignored for very small Reynolds number. x-axis is taken along stretching sheet while y-axis is normal to it (see Figure 1). Velocity of stretching plate is assumed to be proportional to its distance from origin and is given by $u_w = bx$. Fluid on surface of plate is subjected to a nonuniform heat source with internal heat generation rate $\dot{Q}$, heat transfer coefficient h_f, mass transfer coefficient h_m, temperature T_f and concentration C_f. Far free-stream temperature and concentration of fluid are T_∞ and C_∞. Governing continuity, momentum, energy, and concentration equations characterizing flow problems can be described as follows, using these assumptions and boundary layer approximations:

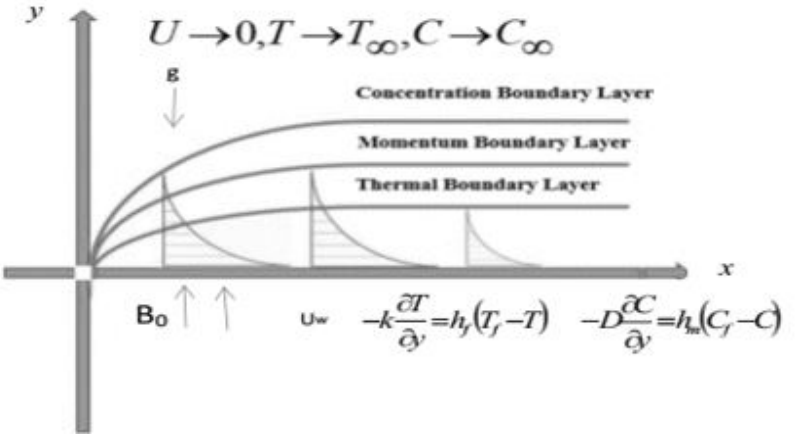

Figure 1: Schematic diagram of the flow.

Assuming the x and y-axes acts along the direction and normal to the surface respectively. Further, if the u and v represent the velocity components in the x and y directions respectively, T being the temperature and C the concentration. The equationsmodelling flow problem becomes:

$$\frac{\partial u}{\partial x} + \frac{\partial v}{\partial y} = 0, \tag{1}$$

$$u\frac{\partial u}{\partial x} + v\frac{\partial u}{\partial y} = \upsilon\frac{\partial^2 u}{\partial y^2} - \lambda_1\left(u^2\frac{\partial^2 u}{\partial x^2} + v^2\frac{\partial^2 u}{\partial y^2} + 2uv\frac{\partial^2 u}{\partial x \partial y}\right) - \frac{\sigma B_0}{\rho}\left(B_0 u + \lambda_1 B_0 v\frac{\partial u}{\partial y}\right)$$
$$-\frac{\upsilon}{k'}u + \beta_T g(T - T_\infty) + \beta_S g(C - C_\infty), \tag{2}$$

$$u\frac{\partial T}{\partial x} + v\frac{\partial T}{\partial y} = \alpha\frac{\partial^2 T}{\partial y^2} + \frac{u}{\rho C_p}\left(\frac{\partial u}{\partial y}\right)^2 + \frac{\sigma B_0^2}{\rho C_P}u^2 + \frac{Q'}{\rho C_p}, \tag{3}$$

$$u\frac{\partial C}{\partial x} + v\frac{\partial C}{\partial y} = D\frac{\partial^2 C}{\partial y^2} + \gamma(C - C_\infty) - \frac{\partial}{\partial y}\left(V_T(C - C_\infty)\right). \tag{4}$$

Subject to the boundary conditions;

$$u(x,0) = bx + q\frac{\partial u}{\partial y}, \quad v(x,0) = -v_w, \quad -k\frac{\partial T}{\partial y} = h_f\left(T_f - T\right),$$

$$-D\frac{\partial C}{\partial y} = h_m\left(C_f - C\right), \quad \text{at} \quad y = 0;$$

$$u(x,\infty) \to 0, \quad \frac{\partial u}{\partial y} \to 0, \quad T(x,\infty) \to T_\infty, \quad \text{as} \quad y \to \infty. \tag{5}$$

Entrenched flow parameters of engineering significance are skin-friction coefficient (C_f), Nusselt value (Nu), and Sherwood value (Sh) that are expressed:

$$C_f = \frac{\tau_w}{\rho u_w^2}, \tag{6}$$

$$Nu = \frac{x q_w}{k(T_w - T_0)}, \tag{7}$$

$$Sh = \frac{x q_m}{D(C_w - C_0)}. \tag{8}$$

In which τ_w, q_w and q_m represent wall shear stress, heat and mass flux, which can be expressed as:

$$\tau_w = \mu \frac{\partial u}{\partial y}\Big|_{y=0}, \tag{9}$$

$$q_w = -k \frac{\partial T}{\partial y}\Big|_{y=0}, \tag{10}$$

$$q_m = -D \frac{\partial C}{\partial y}\Big|_{y=0}. \tag{11}$$

4. Similarity Transformation

Introducing the stream function defined as $\psi(x, y) = \sqrt{bv}xf(\eta)$, and a dimensionless variable $\eta = y\sqrt{\frac{b}{v}}$, the velocity components can be defined in relation to the stream function as in (12) and Equation (1) is satisfy identically by defining the stream function, $\psi(x, y)$ as

$$u = \left(\frac{\partial \psi}{\partial y}\right)_x \quad \text{and} \quad v = \left(\frac{\partial \psi}{\partial x}\right)_y. \tag{12}$$

Equation (12) simplifies to;

$$u = \frac{\partial \psi(x,y)}{\partial y} = bxf'(\eta), \quad v = -\frac{\partial \psi(x,y)}{\partial x} = -\sqrt{bv}f(\eta). \tag{13}$$

Introducing the similarity variables, $T = T_0\theta + T_\infty$, and $C = (C_w - C_\infty)\phi + C_\infty$, into equations (2), (3), (4), and (5) transform into;

$$f'''(\eta) - f'^2(\eta) + f(\eta)f''(\eta) - \lambda(f^2(\eta)f'''(\eta) - 2f(\eta)f'(\eta)f''(\eta))$$
$$-M(f'(\eta) - \lambda f(\eta)f''(\eta)) - Kf'(\eta) + G_T\theta(\eta) + G_S\phi(\eta) = 0, \tag{14}$$

$$\theta'' + Pr\, f(\eta)\theta'(\eta) + Pr\, E\, cf''^2 + Pr\, E\, cMf'^2 + A^* f'(\eta) + B^*\theta(\eta) = 0, \quad (15)$$

$$\phi'' + Pr\, L\, ef(\eta)\phi'(\eta) - Pr\, L\, e\beta\phi(\eta) + Pr\, L\, e\tau(\theta''(\eta)\phi(\eta) + \theta'(\eta)\phi'(\eta)) = 0. \quad (16)$$

Subject to the following constraints:

$$f'(0) = 1 + Q_1 f''(0), \quad f(0) = S, \quad \theta(0) = 1 - S_T + Q_2\theta'(0),$$

$$\phi(0) = 1 - S_C + Q_3\varphi'(0), \quad f'(\infty) \to 0, \quad \theta(\infty) \to 0, \quad \varphi(\infty) \to 0. \quad (17)$$

The Runge Kutta fourth order method and the Newton Raphson Shooting technique were used to estimate the solutions of equations (14) to (17).

5. Results and Discussions

Thermo-physical parameters examined in this research include: Eckert number (Ec), Deborah number (λ), Lewis number (Le), Chemical reaction parameter (β), Biot number (Bi), Magnetic field parameter (M), Solutal Grashof number (G_s), Prandtl number (Pr), Damkohler number (Da), Suction parameter (S), Heat generation parameter (A), Heat generation parameter (B), Thermal Grashof number (G_T), Permeability parameter (K), Momentum slip parameter (Q) and Thermophoretic deposition parameter (τ).

6. Validation of Model

The outcome of the model for skin friction coefficient represented by ($f''(0)$) was compared with the work of Anderson [29] for different values of velocity slip parameter (Q) and for $\lambda = Le = Ec = Bi = M = \beta = G_T = G_S = Da = S = A = B = K = \tau = 0$ and there was excellent agreement with their findings. This validates current model. The comparison is indicated in Table 1.

Table 1: Computational comparison ($f''(0)$) with Anderson [29].

	Anderson [29]	**Current Value**
Q	($\boldsymbol{f''(0)}$)	($\boldsymbol{f''(0)}$)
0.1	-0.8721	-0.8721
0.5	-0.5912	-0.5912
1.0	-0.4302	-0.4302
2.0	-0.2840	-0.2840

7. Impact of Thermophysical Parameters on Coefficient of Skin Friction, Nusselt Number and Sherwood Number

Table 2 shows impact of thermo-physical parameters in coefficient of skin friction $(f''(0))$, Nusselt number representing heat transfer rate $(-\theta'(0))$ and Sherwood number representing mass transfer rate $(-\phi'(0))$. An increase in the Thermophoretic deposition parameter, momentum slip parameter, and Biot number raise Nusselt number but decrease coefficient of skin friction and Sherwood numbers, indicated in the table. In addition, raising Solutal Grashof, thermal Grashof and Damkohler numbers lower skin friction coefficient while raising Nusselt and Sherwood numbers. Raising Eckert number, heat generation parameter A and B lower coefficient of skin friction and Nusselt number while raising Sherwood number. Furthermore, increasing magnetic field parameter, Deborah number, and permeability parameter raise coefficient of skin friction number while lowering Nusselt and Sherwood numbers. Additionally, raising chemical reaction parameter and Lewis number raise coefficient of skin friction and Sherwood number whereas lowering Nusselt number. Finally, raising Prandtl number and Suction parameter simultaneously raise skin friction coefficient, Sherwood and Nusselt numbers.

Table 2: Computationally $(-f''(0))$, $(-\theta'(0))$ and $(-\phi'(0))$ for varying parameter values

T	Le	Da	β	Q	A	B	M	Pr	Bi	Ec	λ	G_T	G_S	S	K	$-f''(0)$	$-\theta'(0)$	$-\phi'(0)$
0.1	0.5	0.1	0.1	0.1	0.1	0.1	0.1	2	0.1	0.1	0.1	0.1	0.1	0.1	0.1	0.999023	0.076314	0.087250
1.0	0.5	0.1	0.1	0.1	0.1	0.1	0.1	2	0.1	0.1	0.1	0.1	0.1	0.1	0.1	0.998360	0.076324	0.086619
2.0	0.5	0.1	0.1	0.1	0.1	0.1	0.1	2	0.1	0.1	0.1	0.1	0.1	0.1	0.1	0.997539	0.076337	0.085904
3.0	0.5															0.996627	0.076352	0.085187
0.1	1.0															1.002132	0.076269	0.091482
	2.0															1.003722	0.076249	0.094358
	3.0															1.004248	0.076244	0.095580
		1.0														0.976760	0.076577	0.407990
		3.0														0.966325	0.076696	0.561890
		5.0														0.963234	0.076730	0.607898
			1.0													1.002431	0.076267	0.092346
			2.0													1.003376	0.076255	0.094062
			3.0													1.003815	0.076250	0.094959
				0.3												0.787645	0.077704	0.086640
				1.0												0.467520	0.078725	0.085357
				2.0												0.302198	0.078231	0.084390
					3.0											0.889488	0.108732	0.088137

					5.0										0.811401	0.245453	0.088699
					7.0										0.733238	0.386858	0.089216
						1.0									0.871218	-0.134341	0.088231
						1.5									0.367777	-1.168406	0.091403
						2.0									-0.391475	-3.098892	0.094706
							0.3								1.070638	0.074910	0.087022
							1.0								1.281706	0.070368	0.086363
							2.0								1.517630	0.064496	0.085667
								3.0							1.004187	0.079996	0.089900
								4.0							1.006682	0.081745	0.091469
								5.0							1.008150	0.082753	0.092525
									1.0						0.984989	0.405730	0.086852
									5.0						0.974321	0.659997	0.086548
									10.0						0.971977	0.716298	0.086476
										0.5					0.983563	0.046208	0.087403
										1.0					0.965180	0.010280	0.087582
										1.5					0.947701	-0.023984	0.087747
											0.01				0.976449	0.076632	0.087344
											0.02				0.978973	0.076597	0.087333
											0.03				0.981492	0.06562	0.087323
												1.0			0.902838	0.077355	0.087546
												3.0			0.718116	0.078872	0.088028
												5.0			0.554685	0.079814	0.088388
													1.0		0.945583	0.076924	0.087432
													2.0		0.890025	0.077488	0.087604
													3.0		0.837548	0.077962	0.087752
														0.14	1.020063	0.077402	0.087629
														0.17	1.036133	0.078164	0.087903
														0.20	1.052462	0.078882	0.088169
															1.0	1.272110	0.072809	0.086397
															2.0	1.501113	0.069096	0.085715
															3.0	1.686641	0.065556	0.085200

7.1. Graphical Result

7.1.1. Variation of parameters on velocity graphs

The impacts of different thermophysical factors on boundary layer's velocity profiles are shown in Figures 2-7. Increases in magnitudes of solutal Grashof number and thermal

Grashof number result in thicker momentum boundary layer thickness, as seen in Figures 2 and 3. In Figures 4-7, increasing Prandtl number, magnetic field parameter, permeability parameters and Deborah numbers reduce fluid's velocity, resulting in thinner momentum boundary layer. Figure 2 shows the velocity graph for solutal Grashof number. As the solutal Grashof number increases, there is a sharp increase close to wall plate, and velocity boundary layer thickness thickens as it agrees with its boundary condition. Similar effects were shown in Figure 3 for the thermal Grashof number. Because Prandtl number is momentum-to-thermal-diffusivity ratio, it reduces velocity of the fluid as Prandtl number rises, as seen in Figure 4. An effect of magnetic field parameter on velocity profile is seen in Figure 5. Velocity of the fluid reduces as magnetic field parameter increases. Because magnetic field retards flow, this result qualitatively follows Lorentz force expectations. Impact of permeability parameter in velocity profile is depicted in Figure 6. As permeability parameter increases, thickness of velocity boundary layer reduces, which is due to an increase in viscosity. Figure 7 shows that increasing Deborah number lowers fluid velocity because relaxation time decreases.

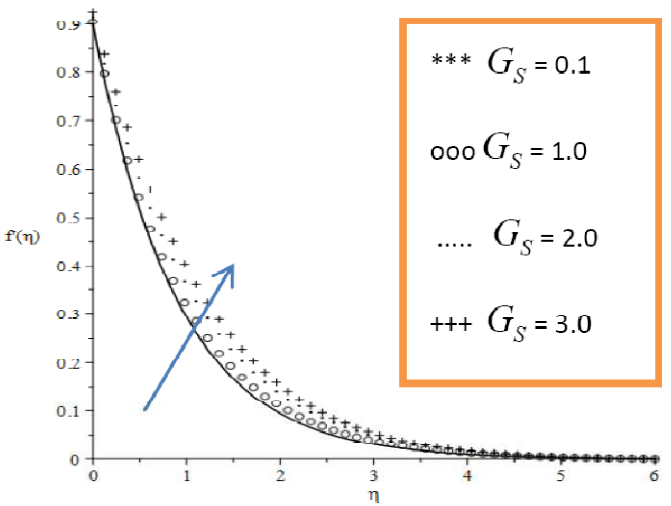

Figure 2: Velocity graph for increasing solutal Grashof number.

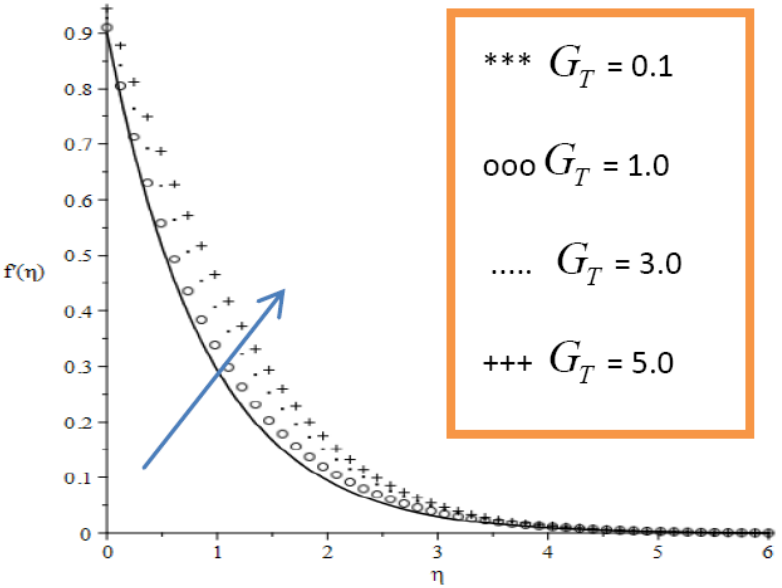

Figure 3: Velocity graph for increasing thermal Grashof values.

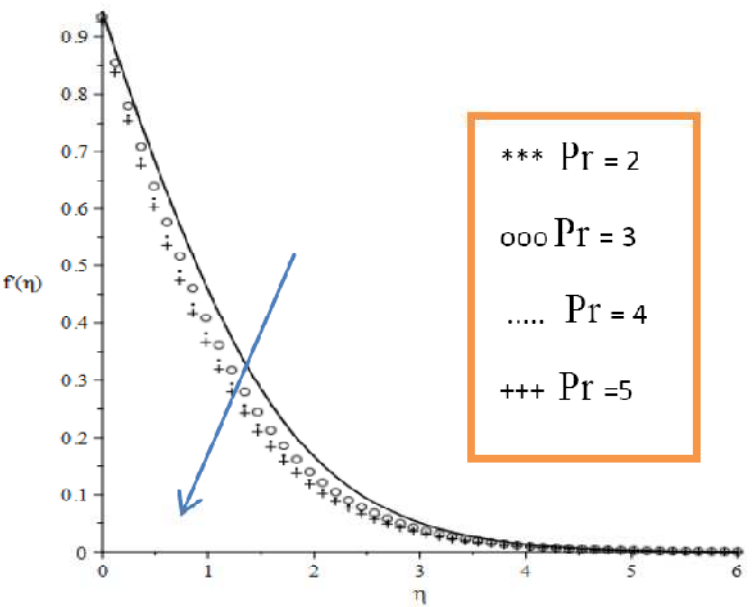

Figure 4: Velocity graph for increasing Prandtl number.

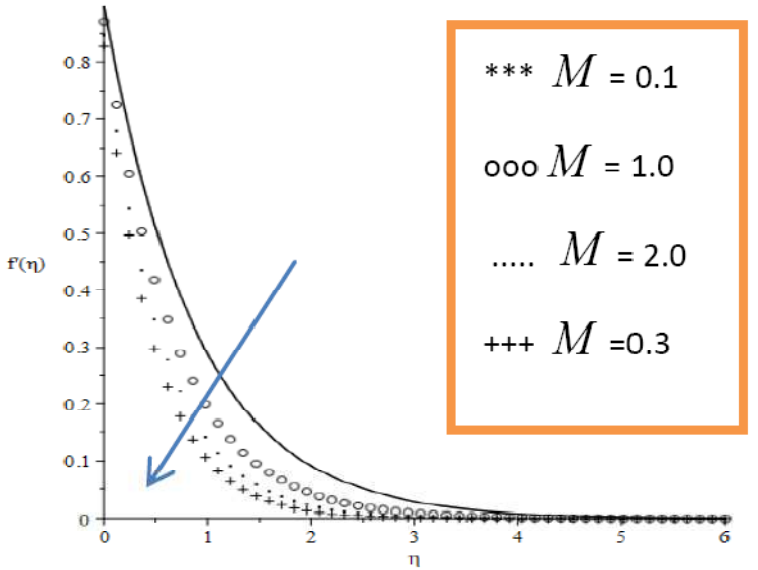

Figure 5: Velocity graph for increasing magnetic field parameters.

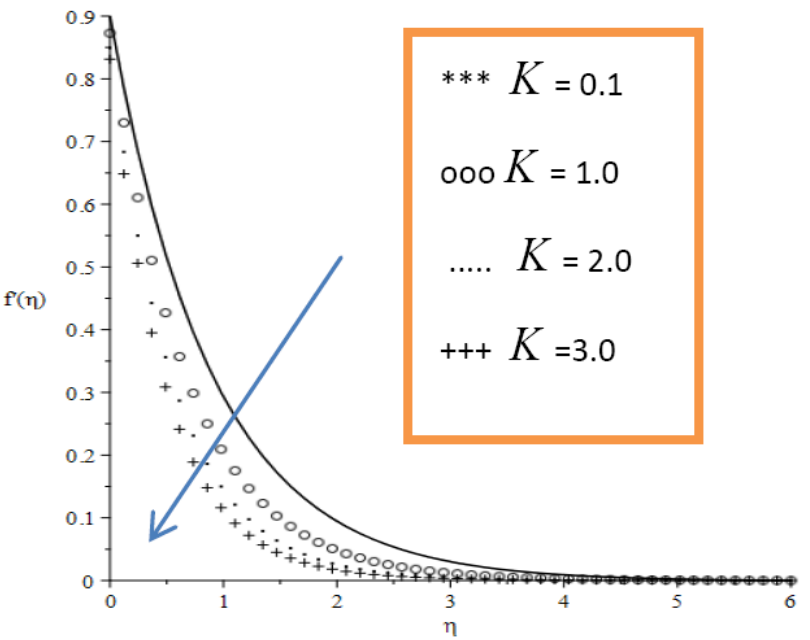

Figure 6: Velocity graph for increasing permeability parameters.

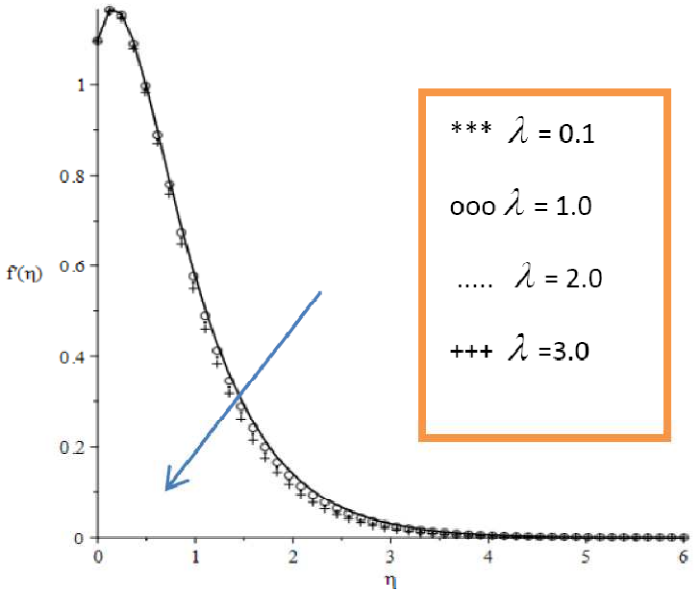

Figure 7: Velocity graph for increasing Deborah numbers.

7.1.2. Variation of parameters on temperature graphs

The effect of different thermophysical parameters on temperature profiles is illustrated in Figures 8-13. Increasing Biot number, permeability parameter, magnetic field parameter and Eckert number as shown in Figures 8-11, raise temperature of fluid and thermal boundary layer become thicker. In Figures 12 and 13, increasing Prandtl number and Thermal Grashof number lower fluid temperature, weakening thermal boundary layer thickness. Biot number increases temperature of fluid base on greater coefficient of heat transmission, as seen in figure 8. Effect of magnetic field parameter on temperature profile is shown in Figure 9. Because of Lorentz force of attraction, thickness of thermal boundary layer has raised result of transverse magnetic field. Figure 10 indicates that increasing permeability parameter increases temperature by increasing thickness of thermal boundary layer, resulting in higher temperature profile. Figure 11 shows that as Eckert number increases, Maxwell fluid temperature and thickness of thermal boundary layer improve due to the rise in kinetic energy. The temperature profile for Prandtl number is shown in Figure 12. When Prandtl number increases, thermally diffusivity is minimized, and temperature decreases. Figure 13 shows that as thermal Grashof number increases, there is a sharp drop towards wall plate, and thermal boundary layer thickness decreases as it conforms to its boundary condition.

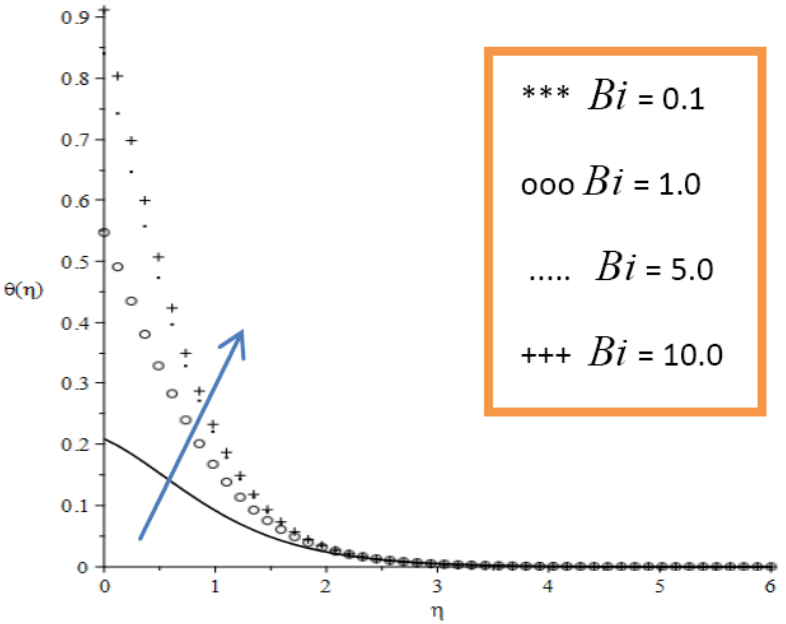

Figure 8: Temperature graph for increasing Biot number.

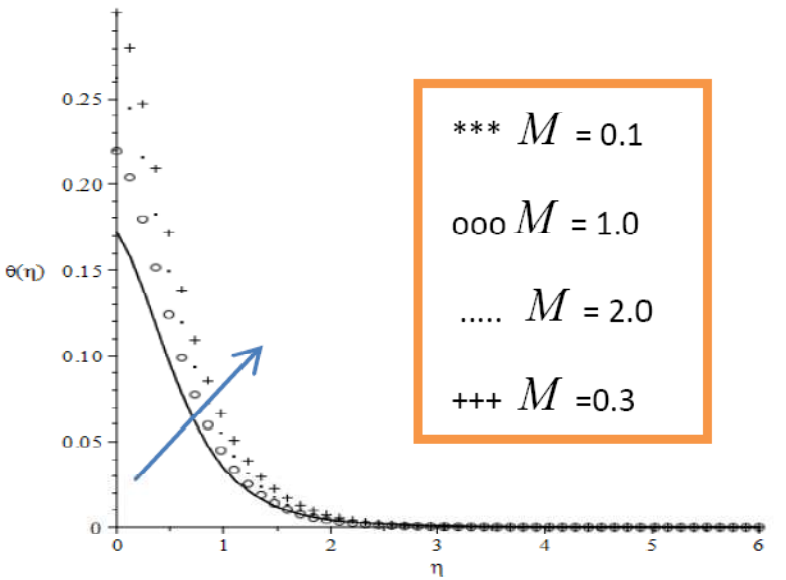

Figure 9: Temperature graph for increasing magnetic field parameters.

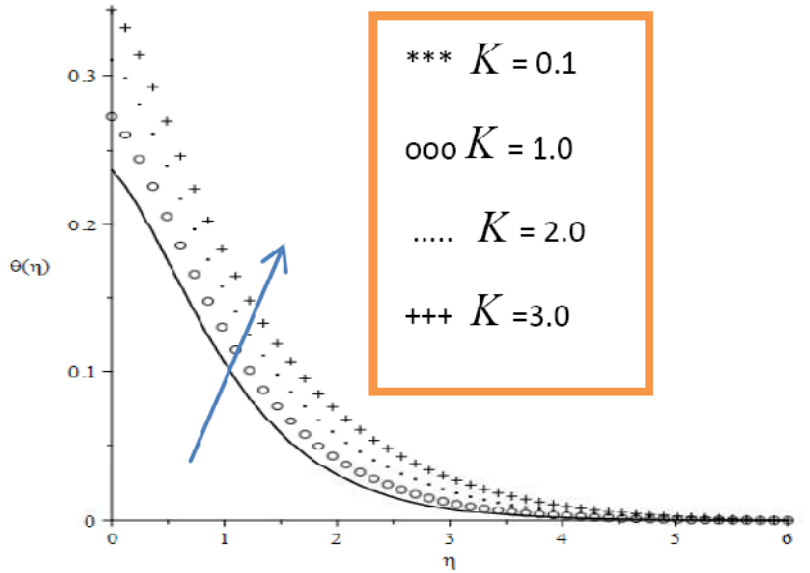

Figure 10: Temperature graph for increasing permeability parameters.

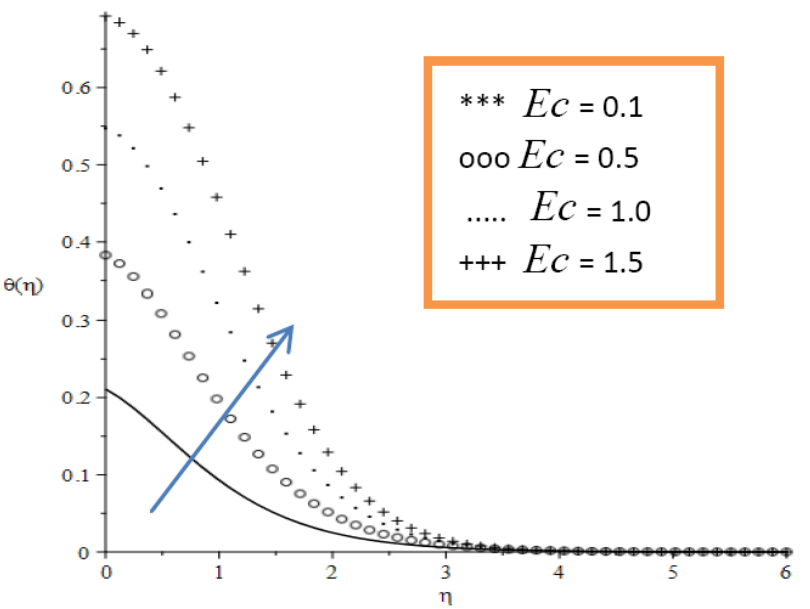

Figure 11: Temperature graph for increasing Eckert numbers.

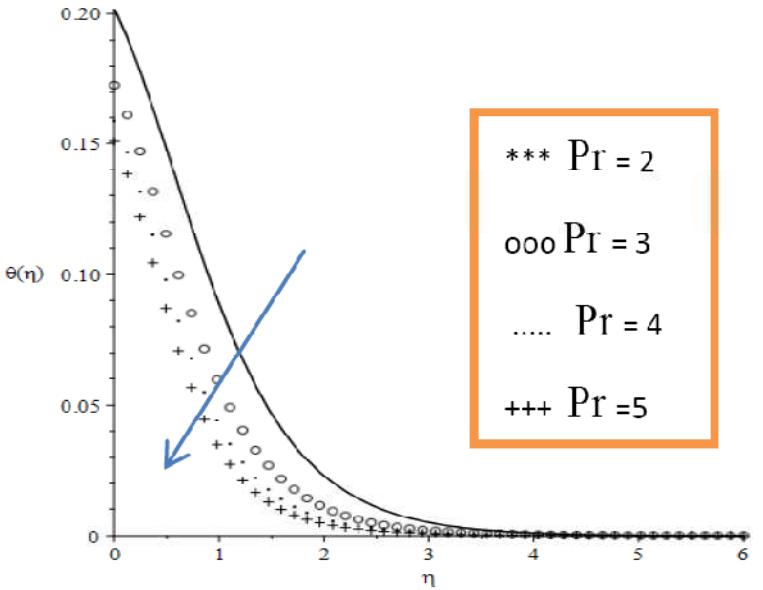

Figure 12: Temperature graph for increasing Prandtl numbers.

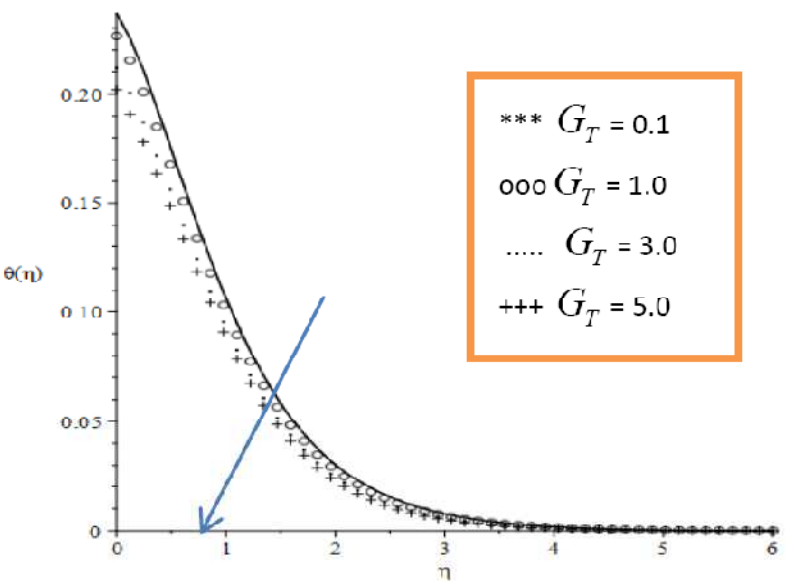

Figure 13: Temperature graph for increasing thermal Grashof numbers.

7.1.3. Variation of parameters on concentration graphs

The effect of changing various thermophysical factors on concentration profiles are indicated in Figures 14-19. Figures 14 and 15 indicate that increasing the thermophoretic deposition parameter and magnetic field parameter increase the fluid concentration, hence increasing thickness of solutal boundary layer. In Figures 16-19, increasing Prandtl number, solutal Grashof number, chemical reaction parameter and Eckert number reduces fluid concentration, resulting in thinner solutal boundary layer. Influence of thermophoretic deposition parameter on concentration profile is indicated in Figure 14. Increases in thermophoretic deposition parameter increases Maxwell fluid particle concentration. Because, thermophoretic deposition depreciates mass transport and amplitudes concentration gradient at the surface. The magnetic field parameter increases concentration result of force induced by Lorentz force of attraction, as shown in Figure 15. The Prandtl number decreases fluid's concentration as shown in Figure 16. Figure 17 shows that as solutal Grashof number increases, fluid concentration near wall plate falls, concentration boundary layer thickness lowers as it agrees with its boundary condition. Impact of chemical reaction parameter on concentration profile is showed in Figure 18. There is a high rate of generating chemical reaction when chemical reaction parameter values are high. The chemical reaction produces more fluid species, causing the concentration of fluid particles to rise. Eckert number reduces concentration of fluid in Figure 19 because there is an enthalpy change that introduces induction heat energy into the fluid thereby lowering concentration boundary layer as shown in the profile.

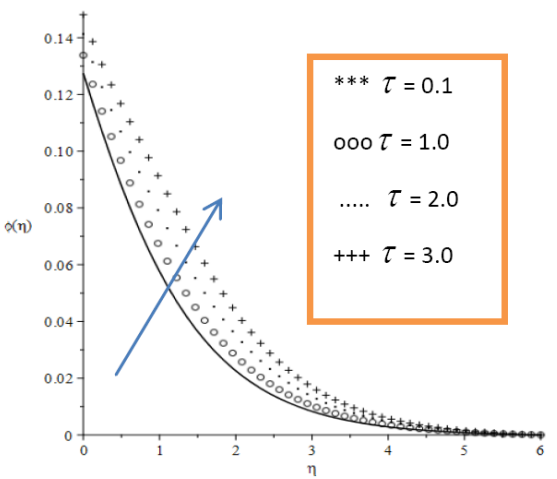

Figure 14: Concentration graphs for increasing Thermophoresis parameter.

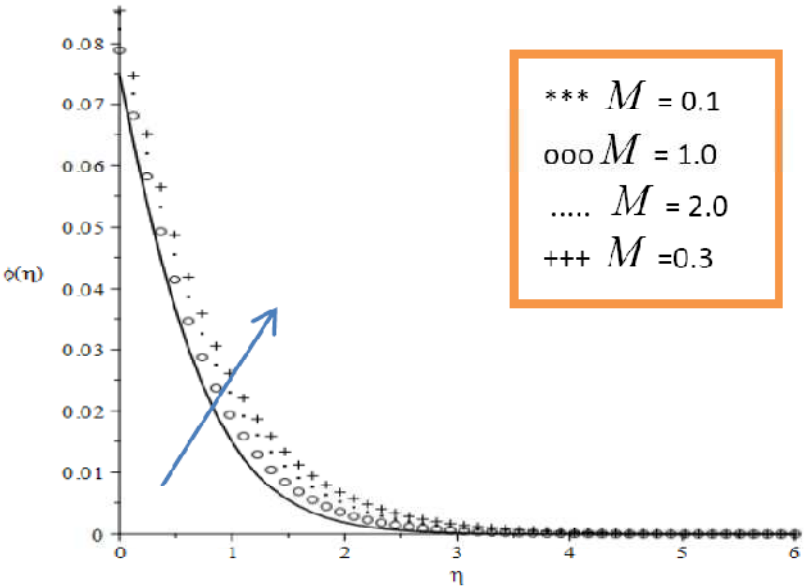

Figure 15: Concentration graphs for increasing magnetic field parameters.

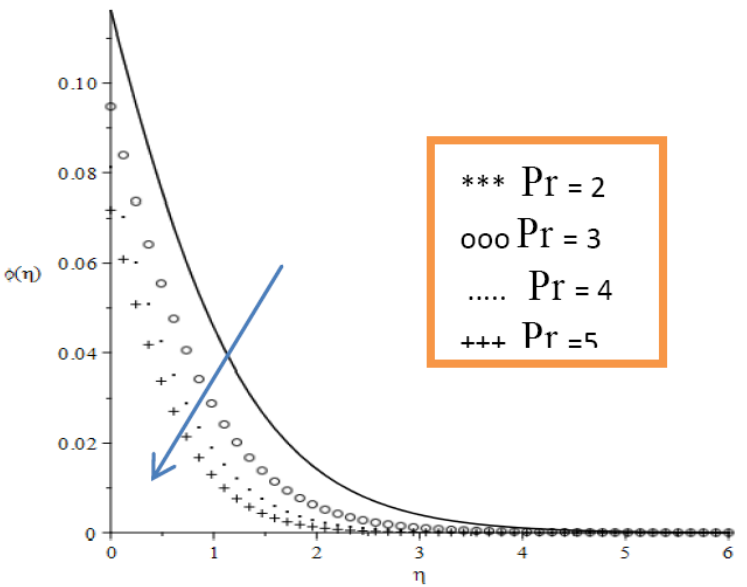

Figure 16: Concentration graphs for increasing Prandtl numbers.

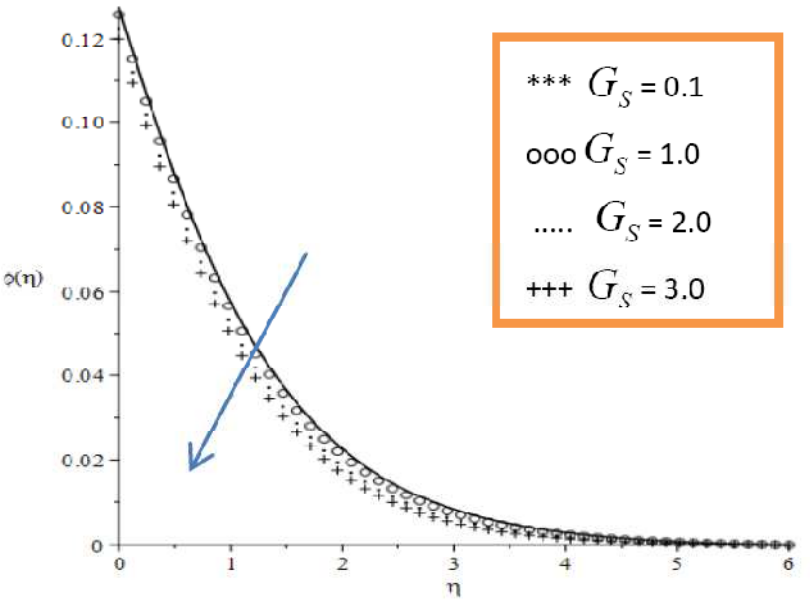

Figure 17: Concentration graphs for increasing solutal Grashof numbers.

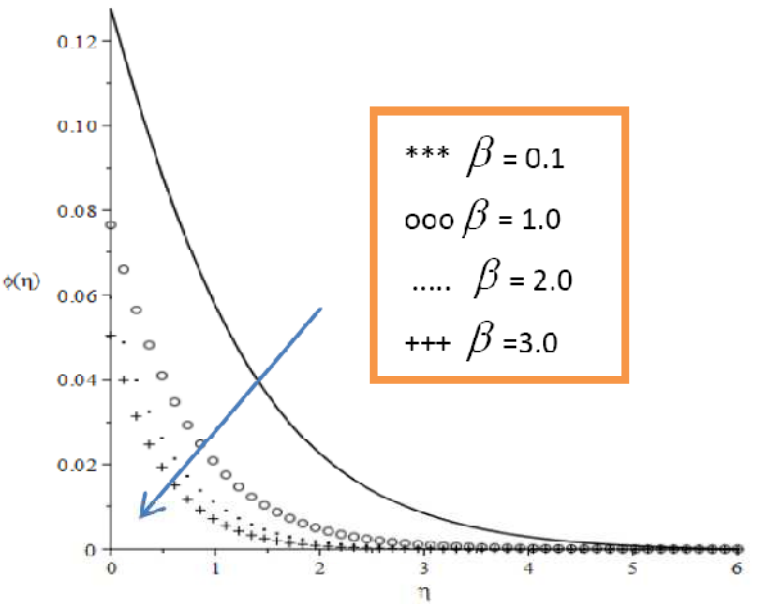

Figure 18: Concentration graphs for increasing Chemical reaction parameters.

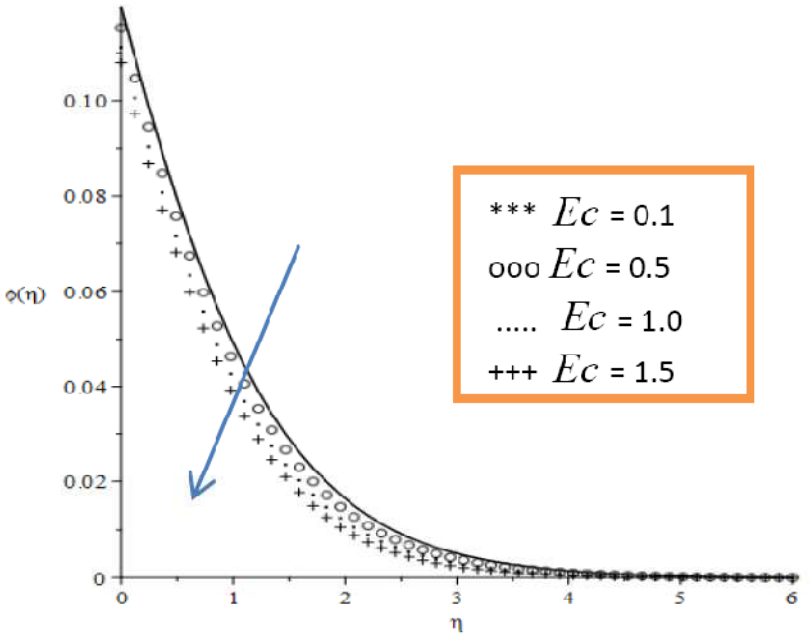

Figure 19: Concentration graphs for increasing Eckert numbers.

8. Conclusion

These study primary findings are summarized as follows:

- Thermophoretic deposition parameter, momentum slip parameter, and Biot number improved heat transfer rate while decreasing skin friction coefficient and rate of mass transfer.
- Increasing Thermal Grashof number, Solutal Grashof number, and Damkohler number reduced coefficient of skin friction number while increasing both mass and heat transfer rates.
- Eckert number, heat generation parameters A and B decreased skin friction coefficient and heat transfer rate while increasing rate of mass transfer.
- Deborah number, magnetic field and permeability parameter increased coefficients skin friction but reduced rate of mass and heat transmission.
- Coefficient of skin friction and mass transfer rate increased with Lewis number and chemical reaction parameter whereas heat transfer rate decreased.

- Damkohler number, Heat generation parameters A and B, Thermal Grashof number, Solutal Grashof number, Biot number, and Eckert number increased momentum boundary layer thickness, whereas Prandtl number, magnetic field parameter, Momentum slip parameter, Permeability parameter, Suction parameter, and Deborah number decreased it.
- Thermal boundary layer became thicker with magnetic field parameter, Momentum slip parameter, Permeability parameter, Biot number, Eckert number, heat generation parameters A and B.
- Solutal boundary layer thickness was increased by increasing Thermophoretic deposition parameter, Damkohler number, Magnetic field parameter, Momentum slip parameter, and Permeability parameter.
- Solutal boundary layer was made thinner by increasing Prandtl number, Lewis number, Solutal Grashof number, Biot number, thermal Grashof number, chemical reaction parameter, heat generation parameters A and B, Suction parameter and Eckert number.

Conflict of Interest

The authors declared no conflicts of interest for the current study, authorship, and publication of this paper.

Funding

The authors did not receive any financial assistance from anywhere for the publication of this paper.

References

[1] Heyhat, M. M., & Khabazi, N. (2011). Non-isothermal flow of Maxwell fluid above fixed flat plates under the influence of a transverse magnetic field. *Journal of Mechanical Engineering Science*, 225(4), 909-916. https://doi.org/10.1243/09544062JMES2245

[2] Mukhopadhyay, S., & Bhattacharyya, K. (2012). Unsteady flow of a Maxwell fluid over a stretching surface in the presence of chemical reaction. *Journal of the Egyptian Mathematical Society*, 20, 229-2394. https://doi.org/10.1016/j.joems.2012.08.019

[3] Zheng, L., Liu, N., & Zhang, X. (2013). Maxwell fluid unsteady mixed flow and radiation heat transfer over boundary slip permeable plate with boundary slip and non-

uniform heat source/sink. *Journal of Heat Transfer*, 135(3), 031705. https://doi.org/10.1115/1.4007891

[4] Ellahi, R., Riaz, A., Abbasbandy, S., Hayat, T., & Vafai, K. (2014). The mixed convention boundary layer flow and heat transfer over a vertical slender cylinder. *Thermal Science*, 18, 1247-1258. https://doi.org/10.2298/TSCI110923097E

[5] Hayat, T., Anwar, M. S., Farooq, M., & Alsaedi, A. (2015). Mixed convection flow of viscoelastic fluid by a stretching cylinder with heat transfer. https://doi.org/10.1371/journal.pone.0118815

[6] Zeeshan, A., Majeed, A., Ellahi, R., & Zia, Q. M. Z. (2018). Mixed convection flow and heat transfer in ferromagnetic fluid over a stretching sheet with partial heat effect. *Thermal Science*, 22(6), 2515-2526. https://doi.org/10.2298/TSCI160610268Z

[7] Krishnaiah, M., Rajendar, P., Laxmi, T. V., & Raddy, M. C. K. (2017). Influence of non-uniform heat source/sink on stagnation point flow of MHD Casson nanofluid flow over an exponentially stretching surface. *Global Journal of Pure and Applied Mathematics*, 13(10), 7009-7033.

[8] Sandeep, N., & Sulochana, C. (2018). Momentum and heat transfer behaviour of Jeffrey, Maxwell and Oldroyer-B nanofluids past a stretching surface with non-uniform heat/sink. *Ain Shams Engineering Journal*, 9(4), 517-524. https://doi.org/10.1016/j.asej.2016.02.008

[9] Abdela, Y., & Shanker, B. (2018). The influence of non-uniform heat source and thermal radiation on MHD stagnation point flow of Maxwell nanofluid over a linear stretching surface. *International Journal of Mathematics Trends and Technology* (*IJMTT*), 56(4), 271-288. https://doi.org/10.14445/22315373/IJMTT-V56P538

[10] Sagheer, M., Shah, S., Hussain, S., & Akhtar, M. (2019). Impact of non-uniform heat source/sink on magnetohydrodynamic Maxwell nanofluid flow over a convective heated stretching face with chemical reaction. *Journal of Nanofluids*, 8(4), 795-805. https://doi.org/10.1166/jon.2019.1622

[11] Dessie, H., & Fissha, D. (2020). MHD mixed convective flow of Maxwell nanofluid past a porous vertical stretching sheet in the presence of chemical reaction. *Applications and Applied Mathematics*, *An International Journal* (*AAM*), 15(1), 530-549.

[12] Hashmi, S. M., Al-Khaled, K., Khan, N., Khan, S. U., & Tlili, T. (2020). Buoyancy-driven mixed convection flow of magnetized Maxwell fluid with homogeneous-heterogeneous reaction with convective boundary condition. *Results in Physics*, 19, 103379. https://doi.org/10.1016/j.rinp.2020.103379

[13] Islam, S., Khan, A., Kuman, P., Alrabaiah, H., Shah, Z., Khan, W., Zubair, M., & Jawad,

M. (2020). Radiative mixed convection flow of Maxwell nanofluid over a stretching cylinder with Joule heating and heat source/sink effect. *Scientific Reports*, 10, 17823. https://doi.org/10.1038/s41598-020-74393-2

[14] Shah, S., & Hussain, S. (2021). Slip effect on mixed convective flow and heat transfer of magnetized UCM fluid through a porous medium in consequence of novel heat flux model. *Results in Physics*, 20, 103749. https://doi.org/10.1016/j.rinp.2020.103749

[15] Aliakbar, V., Alizadah-Pahlavan, A., & Sadeghy, K. (2007). The influence of thermal radiation on MHD Flow of Maxwellian fluids above stretching sheets. *Communications in Nonlinear Science and Numerical Simulation*, 14, 779-794. https://doi.org/10.1016/j.cnsns.2007.12.003

[16] Shateyi, Stanford (2013). A new numerical approach to MHD flow of Maxwell fluid passed vertical stretching sheet in presence of thermophoresis and chemical reaction. *Boundary Value Problems*, 2013, 196. https://doi.org/10.1186/1687-2770-2013-196

[17] Khan, N. A., Sultan, F., & Khan, N. A. (2015). Heat and mass transfer of thermophoretic MHD flow of Powell-Eyring fluid over a vertical stretching sheet in the presence of chemical reaction and joule heating. *International Journal Chemistry Reaction Eng*., 13(1), 37-49. https://doi.org/10.1515/ijcre-2014-0090

[18] Farooq, U., Lu, D., Munir, S., Ranzan, M., Suleman, M., & Hussain, S. (2019). MHD flow of Maxwell fluid with nanomaterial due to an exponentially stretching surface. *Scientific Report*, 9, 7312. https://doi.org/10.1038/s41598-019-43549-0

[19] Chu, Y.-M., Hashmi, M. S., Khan, N. et al. (2020). Thermophoretic particles deposition features in thermally developed flow of Maxwell fluid between two infinite stretching disks. *Journal of Materials Research and Technology*, 9(6), 12889-12898. https://doi.org/10.1016/j.jmrt.2020.09.011

[20] Abo-Eldahab, E. M., & El-Aziz, M. A. (2004). Blowing/suction on hydromagnetic heat transfer by mixed convection from an inclined continuously stretching surface with internal heat generation/absorption. *International Journal of Thermal Science*, 43, 709-719. https://doi.org/10.1016/j.ijthermalsci.2004.01.005

[21] Abiev, R. S. (2022). Mathematical model of two-phase Taylor flow hydrodynamics for four combinations of non-Newtonian and Newtonian fluids in microchannels. *Chemical Engineering Science*, 247, 116930. https://doi.org/10.1016/j.ces.2021.117380

[22] Banerjee, D., Pati, S., & Biswas, P. (2022). Analysis of electroviscous effect and heat transfer for flow of non-Newtonian fluids in a micro-channel with surface charge-dependent slip at high zeta potentials. *Phys. Fluids*, 34, 112016. https://doi.org/10.1063/5.0123964

[23] Alrabaiah, H., Bilal, M., Khan, M. A., Muhammad, T., & Legas, E. Y. (2022). Parametric estimation of gyrotactic microorganism hybrid nanofluid flow between the conical gap of spinning disk-cone apparatus. *Sci. Rep*., 12, 59. https://doi.org/10.1038/s41598-021-03077-2

[24] Madhukesh, J. K., Ramesh, G. K., Aly, E. H., & Chamkha, A. J. (2022). Dynamics of water conveying SWCNT nanoparticles and swimming microorganisms over a Riga plate subject to heat source/sink. *Alexandria Eng. J*., 61, 2418-2429. https://doi.org/10.1016/j.aej.2021.06.104

[25] Azam, M. (2022). Bioconvection and nonlinear thermal extrusion in the development of chemically reactive Sutterby nano-material due to gyrotactic microorganisms. *Int. Commun. Heat Mass Transf*., 130, 105820. https://doi.org/10.1016/j.icheatmasstransfer.2021.105820

[26] Azam, M., Abbas, N., Ganesh Kumar, K., & Wali, S. (2022). Transient bioconvection and activation energy impacts on Casson nanofluid with gyrotactic microorganisms and nonlinear radiation. *Waves Random Complex Media*. https://doi.org/10.1080/17455030.2022.2078014

[27] Waqas, M., Sadiq, M. A., & Bahaidarah, H. M. S. (2022). Gyrotactic bioconvection stratified flow of magnetized micropolar nanoliquid configured by stretchable radiating surface with Joule heating and viscous dissipation. *International Communication Heat Mass Transfer*, 138, 106229. https://doi.org/10.1016/j.icheatmasstransfer.2022.106229

[28] Showkat A. L., Sadia A., Anwar S., & Gabriella B. (2023). A stratified flow of a non-Newtonian Casson fluid comprising microorganisms on a stretching sheet with activation energy, *Scientific Reports*, 13, 11240. https://doi.org/10.1038/s41598-023-38260-0

[29] Anderson, H. I. (2002). Slip flow past a stretching surface. *Acta Mechanica*, 158, 121-125. https://doi.org/10.1007/BF01463174